

### EBX and Mass-Transport Techniques for Phase-Shifted DFB Laser

Sekartedjo Koentjoro, Norikazu Eda,  
Kazuhito Furuya and Yasuharu Suematsu

Department of Physical Electronics  
Tokyo Institute of Technology  
2-12-1 O-okayama, Meguro-ku, Tokyo 152

A method for fabricating phase-shifted DFB laser is presented. The method is a combination between the use of electron beam lithography method for fabrication of corrugation with desired phase-shift and mass-transport technique for reduction of threshold current and facet reflectivity. Low threshold current and stable single mode operation at the Bragg wavelength was measured. This method is convenient since less-complex processes were involved.

#### I. Introduction.

Facing the incoming era of long wavelength optical fiber communication system, the development of the dynamic single mode (DSM) semiconductor laser<sup>1)</sup> as a light source is very important. The DSM laser can operate in single longitudinal mode under high speed modulation, various degree of injection current, and temperature variations.

The phase-shifted DFB laser,<sup>2-6)</sup> that recently developed experimentally<sup>7,8)</sup> in order to solve the 'two modes problem' of conventional DFB laser, is one of the promising DSM lasers. The feature of phase-shifted DFB laser is its ability to operate stably in a single longitudinal mode operation at the Bragg wavelength, which is made possible by introducing a phase shift to the corrugated structure in the middle part of cavity and by reducing reflectivity of facets.

We report here a method for fabrication of phase-shifted DFB laser. The method is a combination between the use of the electron beam lithography for obtaining corrugation with desired phase-shift and the mass-transport technique for reduction of the threshold current

and as well as the effect of facet reflectivity.<sup>9)</sup>

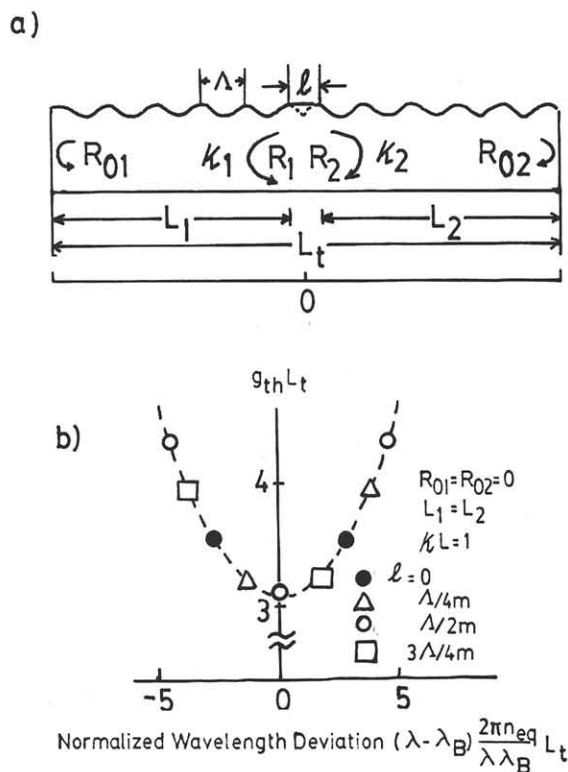


Fig.1. a) schematic diagram of phase-shifted DFB laser  
b) threshold gain vs deviation from Bragg wavelength

## 2. Device Structure.

The schematic diagram of device is shown in Fig.1a. The Bragg wavelength oscillation can be achieved, providing negligible facets reflectivity and  $\Lambda/2m$  ( $\Lambda$  = corrugation pitch,  $m$  = corrugation order) phase shift is introduced in corrugated structure<sup>6)</sup>. This structure leads to the lowest threshold gain in Bragg wavelength while the threshold gain difference between main mode and submode be maximized(Fig.1b) and, therefore, offering stable single mode operation.

The fabricated device structure is shown in Fig. 2, consist of an active region with phase-shifted corrugated structure and mass-transported window regions connected to the ends of cavity.

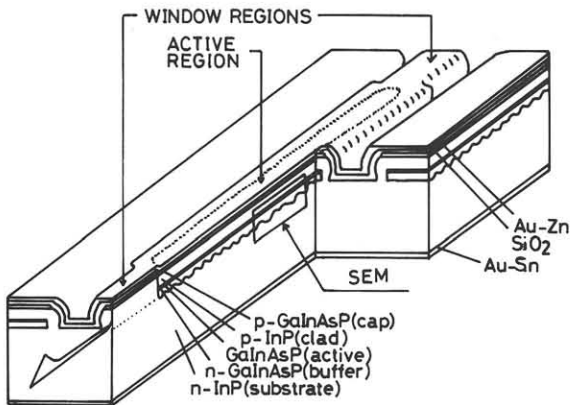


Fig.2. Device structure

## 3. Fabrication process.

### 3.1. Fabrication of corrugation.

The first step in fabrication process is forming the corrugation with phase shift on n-InP substrate. Since it was rather difficult to make a phase shift to the corrugation by conventional laser beam interference method, we employed electron beam lithography method to define the corrugation. The line pitch is  $4630 \text{ \AA}$ , which is corresponds to the 2-nd order grating for lasing at peak photoluminescence wavelength. Since for  $1 \text{ mm}^2$  scanning area the diameter of scanning spot is  $625 \text{ \AA}$ , for  $1.5\text{-}1.6 \mu\text{m}$

range GaInAsP/InP lasers that have pitches of corrugation around  $4600\text{-}4700 \text{ \AA}$ , 8 points is necessary to define the lines. In order to make fine pitch adjustment, an attenuator is inserted between gun deflector and control unit.<sup>10)</sup> OEBR 1000 is used as electron beam resist. The patterns size are  $330 \times 100 \mu\text{m}^2$ , applied voltage is 20kV and

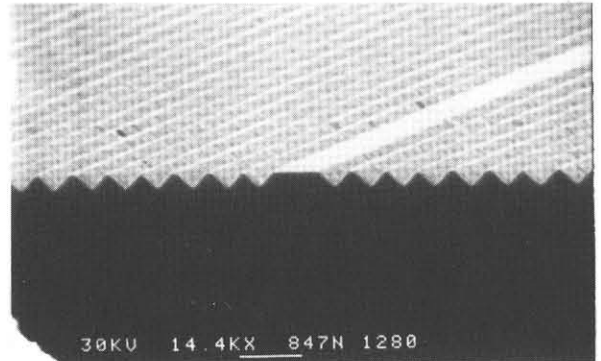


Fig.3. SEM picture of grating profile after etching process

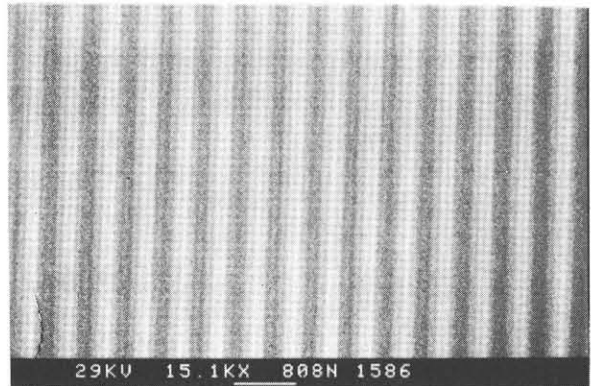


Fig.4. SEM picture of grating obtained by EBX method(top view)

absorption current is  $10^{-10} \text{ A}$ . Scanning speed is  $5 \times 10^4$  points/sec and each pattern are drawn within 45 sec. The pattern was then developed by OEBR developer and transcribed to InP substrate by  $\text{HBr} + \text{HNO}_3 + 10\text{H}_2\text{O}$  etchant. After etching, the grating depth was about  $1500\text{-}2000 \text{ \AA}$ . Fig. 3 shows the SEM picture of grating profile after etching process. As can be seen from Fig.4, uniform and smooth grating was obtained

by EBX method.

### 3.2. Material growth.

After fabrication of corrugation, the  $0.2\mu\text{m}$  thick n-GaInAsP buffer ( $\lambda=1.35\mu\text{m}$ ),  $0.2\mu\text{m}$  thick undoped active ( $\lambda=1.55\mu\text{m}$ ), p-InP clad and p-GaInAsP cap layers were successively grown on the corrugation using LPE technique. The soak and growth temperatures are  $610^\circ\text{C}$  and  $590^\circ\text{C}$ , respectively. Fig.5 shows the SEM picture of layer structure cross-section (marked part of Fig.2) after growth. The grating depth after growth is about  $800\text{-}1000\text{\AA}$ . Interesting to see that after growth, the boundary part of pattern is not perfectly buried with epitaxial layers. This fact was helpful to recognize the pattern,

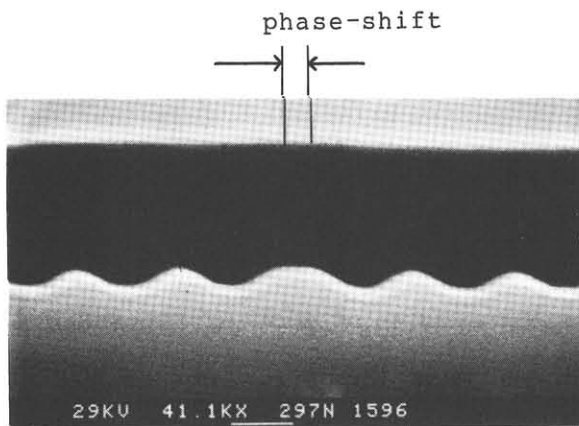


Fig.5. SEM picture of layer structure after growth

which important for proceeding the next process.

### 3.3. Mass-transport technique for reduction of threshold current and facet reflectivity.

Mass-transport technique was recently developed to obtain stable single transverse mode and reduction of threshold current.<sup>11)</sup> As an alternative method instead of conventional BH structure method, the unique feature of mass-transport technique is its simplicity in forming buried structure to

the active layer. In our experiment, we also employed this technique to form the anti-reflecting structure for reduction of facet reflectivity.

First, the  $\text{SiO}_2$  mask was deposited on the wafer. Then, the conventional photolithography and etching method were used to form mesa structure. The mask used to form BH and anti-reflecting structure simultaneously is shown in Fig.6. The active regions consist of  $7\mu\text{m}$  wide and  $300\mu\text{m}$  long sections, which connected to  $5\mu\text{m}$  wide and  $50\mu\text{m}$  long window sections. The etchants

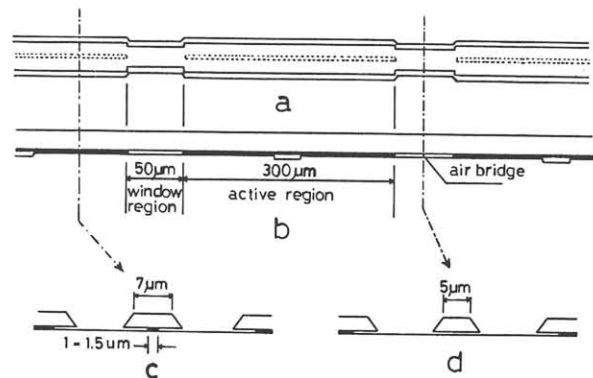


Fig.6. Mask pattern for BH and window region

used for forming the mesa are Br-methanol and  $4\text{HCl}+\text{H}_2\text{O}$ . By observing the etched rate in dummy sections that have the same width as window sections during undercutting process using  $3\text{H}_2\text{SO}_4+\text{H}_2\text{O}+\text{H}_2\text{O}_2$ , we could obtain  $1\text{-}2\mu\text{m}$  active stripes in the active regions (Fig.6c) and air bridges (no active stripes) in window regions (Fig.6d). The mass-transport process were conducted in LPE furnace for 2 hours in  $700^\circ\text{C}$  pure  $\text{H}_2$  atmosphere, producing buried InP either in undercut parts of active region and the air bridges in window regions.

After window stripe opening, Zn-diffusion and evaporation for electrode fabrication, the devices were obtained by cleaving.

About  $25\mu\text{m}$  long of window region

suppressed facet reflectivity to about 1%,<sup>12)</sup> sufficient for obtaining single mode operation.<sup>6)</sup>

#### 4. Lasing characteristics.

As shown in Fig.7, the threshold current of 40mA and several mW/facets of light output power can be achieved. The measured light spectra is also shown. Above threshold, the stable single mode can be observed and below threshold, the

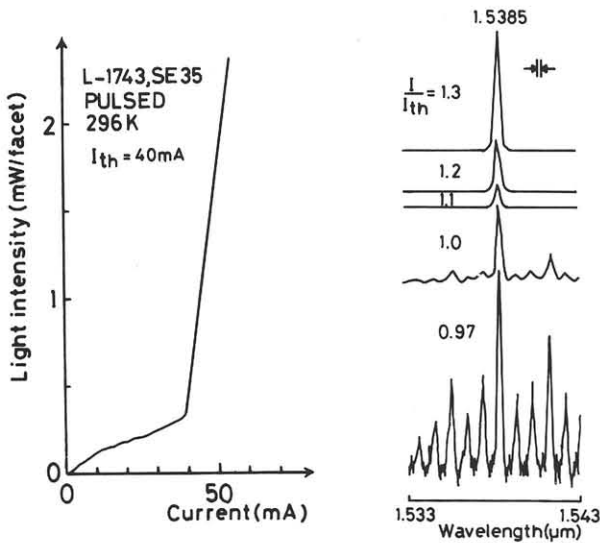


Fig.7. Measured a) I-L characteristic and b) light spectra

symmetrical spectra about the lasing wavelength were measured, indicated that lasing occurred at the Bragg wavelength and therefore, showing the effect of phase-shift introduced to corrugated structure. The measured temperature dependence of lasing wavelength is 0.7Å/K.

#### Conclusion.

We have developed EBX and mass-transport technique for fabricating phase-shifted DFB laser. The low threshold and stable single longitudinal mode operation at the Bragg wavelength was measured. The method is shown very convenient since less-complex processes were involved.

#### Acknowledgement

The authors appreciate Prof.K.Iga for the encouragement. Also helps of Dr. S.Arai in crystal growth experiments, Dr.F.Koyama and Mr.Y.Tohmori in measurements, Mr. B.Broberg and Mr. H.Yamamoto in mask design and fabrication, and Mr. Yoshida in experiments with EBX are highly appreciated. This work was supported by a scientific grant-in aid from the Japanese Ministry of Education, Science and culture and partly by KDD and NTT.

#### References

1. Suematsu, Y., Arai, S., and Kishino, K.: IEEE Lightwave Technol., LT-1(1983)176.
2. Suematsu, Y., and Hayashi, K.: Nat.Conv. Rec. IECE Japan, 1200 (1974)1203.
3. Haus, H.A., and Shank, C.V.: IEEE J. Quant. Electron. QE-12(1976)532.
4. Tada, K., and Suzuki, A.: Monthly Meet. MW Group, IECE Japan, MW77-144(1977).
5. Utaka, K., Akiba, S., Sakai, K., and Matsushima, Y.: Electron.Lett.20(1984) 532.
6. Eda, N., Koentjoro, S., Furuya, K., and Suematsu, Y.: Nat.Conv.Rec.IECE Japan, 984(1984).
7. Sekartedjo, K., Eda, N., Furuya, K., Suematsu, Y., Koyama, F., and Tanbun-Ek, T.: Electron. Lett.20(1984)80.
8. Utaka, K., Akiba, S., Sakai, K., and Matsushima, Y.: Electron.Lett.20(1984) 1008.
9. Broberg, B., Koentjoro, S., Furuya, K., and Suematsu, Y.: Appl.Phys.Lett. July 1985.
10. Furuya, K., Yoshida, K., Honjo, K., and Suematsu, Y.: Trans.IECE Japan, 66(1983) 561.
11. Liau, Z.L., and Walpole, J.N.: Appl.Phys. Lett.40(1982)568.
12. Utaka, K., Akiba, S., Sakai, K., and Matsushima, Y.: IEEE J.Quant. Electron. QE-20(1984)236.